IOP Publishing New J. Phys. 25 (2023) 103048 https://doi.org/10.1088/1367-2630/ad0174

New Journal of Physics
The open access journal at the forefront of physics

Deutsche Physikalische Gesellschaft DPG
IOP Institute of Physics

Published in partnership with: Deutsche Physikalische Gesellschaft and the Institute of Physics

OPEN ACCESS

RECEIVED
23 August 2023

REVISED
30 September 2023

ACCEPTED FOR PUBLICATION
9 October 2023

PUBLISHED
25 October 2023

PAPER

Quantum phase transitions in the anti-Jaynes-Cummings triangle model

Jia-Ming Cheng[1], **Yong-Chang Zhang**[2,*], **Xiang-Fa Zhou**[3,4,5,*] **and Zheng-Wei Zhou**[3,4,5,*]

1 Xi'an Microelectronics Technology Institute, Xi'an 710065, People's Republic of China
2 MOE Key Laboratory for Nonequilibrium Synthesis and Modulation of Condensed Matter, Shaanxi Key Laboratory of Quantum Information and Quantum Optoelectronic Devices, School of Physics, Xi'an Jiaotong University, Xi'an 710049, People's Republic of China
3 CAS Key Lab of Quantum Information, University of Science and Technology of China, Hefei 230026, People's Republic of China
4 Synergetic Innovation Center of Quantum Information and Quantum Physics, University of Science and Technology of China, Hefei 230026, People's Republic of China
5 Hefei National Laboratory, University of Science and Technology of China, Hefei 230088, People's Republic of China
* Authors to whom any correspondence should be addressed.

E-mail: zhangyc@xjtu.edu.cn, xfzhou@ustc.edu.cn and zwzhou@ustc.edu.cn

Keywords: continuous $U(1)$ symmetry, superradiant phase, artificial gauge field, chiral photon current

Abstract

We carefully investigate the comprehensive impact of atom-cavity interaction and artificial magnetic fields on quantum phase transitions of anti-Jaynes-Cummings triangle model in the infinite frequency limit. We discover that ground states of the optical field can be a gapped normal phase (NP) or three kinds of gapless superradiant phases with infinite degeneracy. When the atom-cavity coupling is weak, the optical field is in a NP, which is a vacuum with no photons. Otherwise, it will stay at one of the superradiant phases: a normal superradiant phase without photon currents and another two chiral superradiant phases with opposite photon currents. The former only breaks the continuous $U(1)$ symmetry and its gapless excitations are normal Goldstone modes. Nevertheless, the latter, mainly induced by an external synthetic gauge field, break both the continuous $U(1)$ symmetry and chiral symmetry, thereby corresponding gapless excitations are chiral Goldstone modes. In addition, we also propose a detecting scheme to distinguish these superradiant phases.

1. Introduction

With a view to the potential applications of novel quantum states in quantum technologies [1, 2], such as quantum computation and quantum metrology [3, 4], the search for exotic quantum matters has always been a rapidly growing topic in fields of condensed matter physics and quantum simulations in the past decades [5–9]. Up until now, exotic quantum phases either predicted theoretically or realized in experiments include superfluids and Mott insulators [10, 11], topological insulators [12, 13], topological superconductors [14, 15], quantum Hall states [16, 17], spin textures [18–20], Majorana zero modes [21–23], and so on.

Appearances of these quantum states are usually accompanied by quantum phase transitions (QPTs) or topological QPTs, during which an order parameter or a topological invariant will change [24–27]. In Landau theory, spontaneous symmetry breaking and energy gap closing are the two typical characteristics in a continuous QPT [28], which results from the comprehensive interplay of intrinsic symmetries, particle interactions, external gauge field, etc. For example, for Dicke model implemented in cavity quantum electrodynamics (QEDs) or circuit QED, it was predicted to experience a superradiant phase transition that breaks the $\mathbf{Z}_2$ symmetry if its atom-cavity interaction can exceed a threshold value [29–32]; synthetic gauge fields contribute to the emergence of Bose–Einstein condensates with non-zero momentum or angular momentum in ultra-cold atoms [33, 34]. The common point of these QPTs is that they generally happen in a many-body system under the thermodynamical limit [25]. However, it was theoretically suggested that a QPT can also come out in few-body systems by taking the Rabi model as an example [35], which was observed in an experiment with a single trapped ion [36]. Here the original thermodynamical limit is replaced by a frequency limit, that is, an infinite ratio of atomic transition frequency to cavity field frequency is required. Motivated by the easy manipulations, few-body systems turn out to be interesting and can be utilized to simulate many-body strongly-correlated systems [37, 38]. Recently, chiral photon currents are detected with a three-qubit loop in a synthetic magnetic field [39], as well as are predicted to exist in a Rabi triangle model by adjusting artificial gauge fields [40]. Furthermore, the Rabi triangle model can be mapped into an effective magnetic model containing the XY exchange and Dzyaloshinskii Moriya interactions [41], which is useful for the study of topological phenomena in spin systems.

In this article, we explore the quantum ground states of an anti-Jaynes-Cummings (aJC) triangle model under the combined actions of atom-cavity interaction and artificial magnetic fields. Based on analytic approaches and numerical variation methods, we find out its quantum phase diagram in the infinite frequency limit. The cavity field is in a gapped normal phase (NP) possessing no photons when the atom-cavity coupling is weak; otherwise, it would rather remain at one of three superradiant phases breaking the continuous $U(1)$ symmetry. We classify these novel states as normal superradiant phase (NSP) or chiral superradiant phase (CSP) depending on whether or not a photon current exists. Induced by an external synthetic gauge field, the CSPs have a non-zero photon current and also beak the chiral symmetry. All the three SPs are gapless with infinite degeneracy. Besides, a method is elaborated to successfully detect the NSP and CSPs in strong atom-cavity coupling.

This paper is organized as follows. In section 2, we introduce Hamiltonian of the aJC triangle model. We next derive effective Hamiltonians of the optical field in cases of both weak and strong atom-cavity interactions in section 3. Subsequently, we present the phase diagram and discuss NP and SPs as well as their spontaneous symmetry breaking in section 4. We also design a detecting scheme to discriminate these superradiant phases in section 5. At last, we conclude this article in section 6. Technical details can be found in the appendices.

2. Anti-Jaynes-Cummings triangle model

We consider quantum ground states of the aJC triangle model that is composed of three identical optical cavities as illustrated in figure 1. Each cavity can store a two-level atom with transition frequency Ω and a single-mode optical field with frequency ω. Photons can interact with the atom in each cavity, and hop between adjacent cavities forming a closed loop. We suppose this atom-cavity interaction to be the aJC-type, which does not appear naturally in cavity QED. However, the aJC-type interaction can be brought about in trapped-ion systems by tuning laser frequencies close to the blue sideband [42–44]. Hence the aJC triangle model can be accomplished through leveraging trapped ions [45]. Hamiltonian of this setup can be described as

$$H=\sum_{n=1}^{3}\left[\frac{\hbar\Omega}{2}\sigma_n^z+\hbar\omega a_n^\dagger a_n+\frac{\hbar g}{2}\left(a_n^\dagger\sigma_n^\dagger+a_n\sigma_n^-\right)+\left(te^{i\theta}a_n^\dagger a_{n+1}+\mathrm{h.c.}\right)\right], \tag{1}$$

where $\sigma_n^+=(\sigma_n^-)^\dagger=|e\rangle_n\langle g|$ and Pauli matrix $\sigma_n^z=|e\rangle_n\langle e|-|g\rangle_n\langle g|$ describe operations on an atom in the nth cavity, a_n and $a_n^\dagger$ denote the photonic annihilation and creation operators, g represents strength of the aJC-type interaction between itinerant photons and atoms, t stands for the hopping strength of photons and $\hbar$ is the reduced Planck constant. When photons tunnel between neighboring cavities, a phase $\theta=\int_{r_n}^{r_{n+1}}A(r)\mathrm{d}r$ is picked up due to existence of a (synthetic) magnetic field with vector potential $A(r)$ [46, 47]. The artificial gauge field can be implemented by a Floquet modulation method [39, 40]. In the aJC-triangle model, total number of excitation

$$N_e=\sum_{n=1}^{3}\left(a_n^\dagger a_n-\sigma_n^\dagger\sigma_n^-\right) \tag{2}$$

is invariant because $[N_e,H]=0$. That is, Hamiltonian H is invariant under the global gauge transformation $\mathcal{U}(\phi)=\exp(i\phi N_e)$, which will give rise to a continuous $U(1)$ symmetry. According to the Goldstone theorem, its spontaneous symmetry breaking would lead to the appearance of gapless Goldstone modes [48, 49].

3. Effective Hamiltonian of the optical field

We investigate QPT in the frequency limit $\Omega/\omega\to\infty$ and mainly consider low energy physics in case of $\hbar\omega\gg t$. Therefore, in this aJC triangle model, the atomic transition energy $\hbar\Omega$ is dominated. The two-level

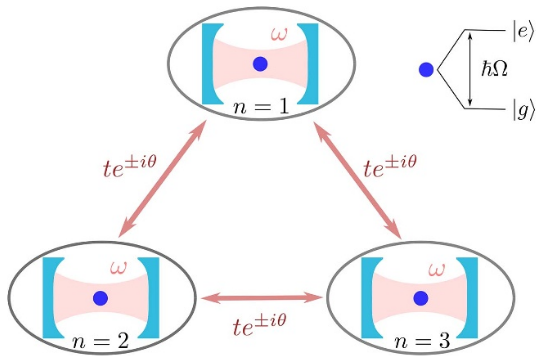

Figure 1. Schematic diagram of the aJC triangle model. It consists of three uniform optical cavities with photon frequency ω. A two-level atom resides in each cavity and can interact with the intracavity photons. Transition frequency of the two-level atom is Ω. Photons can tunnel between adjacent cavities forming a closed loop. The complex tunneling strength is labeled as $te^{\pm i\theta}$.

atom in each cavity will stay at its ground state in weak atom-cavity coupling or fluctuate around it when the coupling is strong. In contrast, the optical field would exhibit novel quantum states under different situations.

For weak on-site coupling g, we first need to make a Schrieffer–Wolff transformation

$$U_1 = \exp\left[-\frac{g}{2(\Omega+\omega)}\sum_{n=1}^{3}\left(a_n^\dagger\sigma_n^\dagger - a_n\sigma_n^-\right)\right]. \tag{3}$$

To second order of g, the transformed Hamiltonian $H_1 = U_1^\dagger H U_1$ has following form

$$H_1 \approx \sum_{n=1}^{3}\left[\frac{\hbar}{2}\Omega\sigma_n^z + \hbar\omega(1+\frac{g^2}{g_0^2}\sigma_n^z)a_n^\dagger a_n + \frac{\hbar\omega}{2}\frac{g^2}{g_0^2}(\sigma_n^z-1) + t(\mathrm{e}^{i\theta}a_n^\dagger a_{n+1} + \mathrm{e}^{-i\theta}a_{n+1}^\dagger a_n)\right] \tag{4}$$

in the frequency limit $\Omega/\omega\to\infty$ (see also equation (A.7)). Here we have defined a new parameter $g_0 = 2\sqrt{\Omega\omega}$. As transition frequency of the two-level atom is dominated ($\Omega\gg\omega\gg t/\hbar$), atoms should stay at their ground states $|0\rangle_\sigma = \prod_{n=1}^{3}|g\rangle_n$. Physical behaviors of the optical field are governed by Hamiltonian $H_{np} = \langle 0|H_1|0\rangle_\sigma$, whose concrete form becomes

$$H_{np} = -\frac{3}{2}\hbar\left(\Omega+2\omega\frac{g^2}{g_0^2}\right) + \sum_{n=1}^{3}\left[\hbar\omega\left(1-\frac{g^2}{g_0^2}\right)a_n^\dagger a_n + t\left(\mathrm{e}^{i\theta}a_n^\dagger a_{n+1} + \mathrm{h.c.}\right)\right]. \tag{5}$$

Due to existence of the periodic boundary condition, we next make a Fourier transformation to the momentum space

$$a_n = \frac{1}{\sqrt{3}}\sum_p \mathrm{e}^{-inp}a_p \tag{6}$$

with $p = 0, \pm\frac{2}{3}\pi$. Hamiltonian H_{np} can now be rewritten as

$$H_{np} = \sum_p \xi_{np}(p)\, a_p^\dagger a_p - \frac{3}{2}\hbar\left(\Omega+2\omega\frac{g^2}{g_0^2}\right) \tag{7}$$

with $\xi_{np}(p) = \hbar\omega(1-\frac{g^2}{g_0^2}) + 2t\cos(\theta-p)$, from which we can realize that it is valid only when the on-site coupling is weak $g<g_0$ and tunneling t is small enough such that we can always have $\xi_{np}(p)\geqslant 0$ for any p and $\theta\in(-\pi,\pi)$. In our numerical calculation, we set $t=0.1\hbar\omega$. In the original frame, its ground state can be presented as

$$|\psi\rangle_{np} = U_1|0\rangle_a|0\rangle_\sigma \tag{8}$$

with $a_p|0\rangle_a = 0$. From equation (3), it can be known that this ground state $|\psi\rangle_{np}$ is dependent on the atom-field interaction g. Its corresponding energy is $E_{np} = -\frac{3}{2}\hbar(\Omega+2\omega\frac{g^2}{g_0^2})$. This state indicates that there exists no photon and all atoms are at their ground states. So we can name it as NP. As g increase across some value, instability occurs when we have $\xi_{np}(p) < 0$. Thus QPT will take place when the on-site coupling g is strong enough.

For strong on-site coupling g, the optical field can not remain in a vacuum state any longer. We need to make a local translation to the cavity field

$$D = \exp\left[\sum_{n=1}^{3}\left(\alpha_n a_n^\dagger - \alpha_n^* a_n\right)\right] \tag{9}$$

with complex parameter $\alpha_n = |\alpha_n| e^{i\gamma_n}$, and can get a translated Hamiltonian $H_2' = D^\dagger H D$. Then this new Hamiltonian H_2' reads (see equation (A.10))

$$\begin{aligned} H_2' = \sum_{n=1}^{3}\Big[&\hbar\omega|\alpha_n|^2 + (te^{i\theta}\alpha_n^*\alpha_{n+1} + \text{c.c}) + \frac{\hbar}{2}\Omega\sigma_n^z + \hbar\omega a_n^\dagger a_n \\ &+ \frac{\hbar g}{2}(a_n^\dagger\sigma_n^\dagger + \alpha_n^*\sigma_n^\dagger + \text{h.c.}) + t(e^{i\theta}a_n^\dagger a_{n+1} + \text{h.c.}) \\ &+ [(\hbar\omega\alpha_n + te^{i\theta}\alpha_{n+1} + te^{-i\theta}\alpha_{n-1})a_n^\dagger + \text{h.c.}]\Big]. \end{aligned} \tag{10}$$

To clarify clearly effects of the local translation α_n, it can be helpful to apply a unitary transformation

$$U = \exp\left[i\sum_{n=1}^{3}\gamma_n\left(a_n^\dagger a_n - \sigma_n^\dagger\sigma_n^-\right)\right]. \tag{11}$$

We will get a new translated Hamiltonian $\mathcal{H}_2' = U^\dagger H_2' U$ and know that

$$\begin{aligned} \mathcal{H}_2' = \sum_{n=1}^{3}\Big[&\hbar\omega|\alpha_n|^2 + 2t\cos\theta_n|\alpha_n||\alpha_{n+1}| + H_{qn} + \hbar\omega a_n^\dagger a_n \\ &+ \frac{\hbar g}{2}(a_n^\dagger\sigma_n^\dagger + a_n\sigma_n^-) + t(e^{i\theta_n}a_n^\dagger a_{n+1} + \text{h.c.}) \\ &+ [(\hbar\omega|\alpha_n| + te^{i\theta_n}|\alpha_{n+1}| + te^{-i\theta_{n-1}}|\alpha_{n-1}|)a_n^\dagger + \text{h.c.}]\Big] \end{aligned} \tag{12}$$

with phase $\theta_n = \theta + \gamma_{n+1} - \gamma_n$ and a local atomic Hamiltonian

$$H_{qn} = \frac{\hbar}{2}\Omega\sigma_n^z + \frac{\hbar g}{2}|\alpha_n|\sigma_n^x. \tag{13}$$

It is needed to note that the continuous $U(1)$ symmetry is manifested in freedom of selecting phase γ_n: Hamiltonian $\mathcal{H}_2'$ is invariant under a phase shift $\gamma_n \to \gamma_n + \phi$. From equation (12), we can realize that if there are photons in cavities, on one hand, they may induce an effective tunneling phase θ_n; on the other hand, they can perturb an atom in the nth cavity away from its ground state $|g\rangle_n$. As to this two-level atom, its Hamiltonian H_{qn} can be diagonalized as $H_{qn} = \frac{\hbar}{2}\Omega_n\tau_n^z$ with $\Omega_n = \sqrt{\Omega^2 + g^2|\alpha_n|^2}$ and $\tau_n^z = |+\rangle_n\langle+| - |-\rangle_n\langle-|$. In its eigenstates bases, Hamiltonian $\mathcal{H}_2'$ can be changed into (see equation (A.17))

$$\begin{aligned} \mathcal{H}_2' = \sum_{n=1}^{3}\Bigg[&\left(\left[\left(\frac{\hbar g^2}{4\Omega_n}\tau_n^z + \hbar\omega\right)|\alpha_n| + te^{i\theta_n}|\alpha_{n+1}| + te^{-i\theta_{n-1}}|\alpha_{n-1}|\right]a_n^\dagger + \text{h.c.}\right) \\ &- \frac{\hbar g}{4}\left[\left(1 + \frac{\Omega}{\Omega_n}\right)(a_n^\dagger\tau_n^\dagger + a_n\tau_n^-) - \left(1 - \frac{\Omega}{\Omega_n}\right)(a_n^\dagger\tau_n^- + a_n\tau_n^\dagger)\right] \\ &+ \frac{\hbar}{2}\Omega_n\tau_n^z + \hbar\omega a_n^\dagger a_n + t(e^{i\theta_n}a_n^\dagger a_{n+1} + \text{h.c.}) \\ &+ (\hbar\omega|\alpha_n|^2 + 2t\cos\theta_n|\alpha_n||\alpha_{n+1}|)\Bigg]. \end{aligned} \tag{14}$$

As atomic energy $\hbar\Omega_n$ is predominant in Hamiltonian $\mathcal{H}_2'$, it is valid to assume that the atom in each cavity would keep occupying its ground state $|-\rangle_n$. The first line in equation (14) can be eliminated by demanding that

$$\left(\hbar\omega - \frac{\hbar g^2}{4\Omega_n}\right)|\alpha_n| + te^{i\theta_n}|\alpha_{n+1}| + te^{-i\theta_{n-1}}|\alpha_{n-1}| = 0. \tag{15}$$

Under this situation, Hamiltonian $\mathcal{H}_2'$ becomes

$$\mathcal{H}_2' = \sum_{n=1}^{3} \left[\frac{\hbar g}{4} \left[\left(1 - \frac{\Omega}{\Omega_n}\right)(a_n^\dagger \tau_n^- + a_n \tau_n^\dagger) - \left(1 + \frac{\Omega}{\Omega_n}\right)(a_n^\dagger \tau_n^\dagger + a_n \tau_n^-) \right] + \frac{\hbar}{2}\Omega_n \tau_n^z + \hbar\omega a_n^\dagger a_n + t(\mathrm{e}^{i\theta_n} a_n^\dagger a_{n+1} + \mathrm{h.c.}) + (\hbar\omega|\alpha_n|^2 + 2t\cos\theta_n |\alpha_n||\alpha_{n+1}|) \right], \tag{16}$$

which can be diagonalized by another Schrieffer–Wolff transformation $U_2 = \mathrm{e}^{-S_2}$ with

$$S_2 = \sum_{n=1}^{3} \frac{g}{4} \left[\frac{1 - \frac{\Omega}{\Omega_n}}{\Omega_n - \omega}(a_n \tau_n^\dagger - a_n^\dagger \tau_n^-) - \frac{1 + \frac{\Omega}{\Omega_n}}{\Omega_n + \omega}(a_n^\dagger \tau_n^\dagger - a_n \tau_n^-) \right]. \tag{17}$$

We mark the diagonalized Hamiltonian as H_2 and in the limit of $\Omega/\omega \to \infty$, it becomes

$$H_2 \approx \sum_{n=1}^{3} \left[\hbar\omega|\alpha_n|^2 + 2t\cos\theta_n|\alpha_n||\alpha_{n+1}| - \frac{\hbar\omega}{2}\frac{g^2\Omega}{g_0^2\Omega_n} + \frac{\hbar}{2}\Omega_n\tau_n^z + \hbar\omega a_n^\dagger a_n + t(\mathrm{e}^{i\theta_n} a_n^\dagger a_{n+1} + \mathrm{h.c.}) + \frac{\hbar\omega}{4}\frac{g^2\Omega}{g_0^2\Omega_n}\left[\left(1 + \frac{\Omega^2}{\Omega_n^2}\right)(2a_n^\dagger a_n + 1)\tau_n^z - \left(1 - \frac{\Omega^2}{\Omega_n^2}\right)(a_n^{\dagger 2} + a_n^2)\tau_n^z \right] \right] \tag{18}$$

to second order of on-site coupling g (see equation (A.24)). Hamiltonian of the cavity field can be defined as $H_{\mathrm{sp}} = \langle -|H_2|-\rangle_\sigma$ with $|-\rangle_\sigma = \prod_{n=1}^{3} |-\rangle_n$, which can be in form of

$$H_{sp} = \sum_{n=1}^{3} \hbar\omega \left[\frac{1}{2}(1 - \lambda_n^+)(a_n^\dagger a_n + a_n a_n^\dagger) + \frac{1}{2}\lambda_n^-(a_n^{\dagger 2} + a_n^2) + t'(\mathrm{e}^{i\theta_n} a_n^\dagger a_{n+1} + \mathrm{h.c.}) \right] + E \tag{19}$$

with dimensionless parameters $\lambda_n^\pm = \frac{1}{2}\frac{g^2\Omega}{g_0^2\Omega_n}(1 \pm \frac{\Omega^2}{\Omega_n^2})$, $t' = \frac{t}{\hbar\omega}$ and undetermined energy

$$E = \sum_{n=1}^{3} \left[\hbar\omega\left(|\alpha_n|^2 - \frac{1}{2} - \frac{1}{2}\frac{g^2\Omega^2}{g_0^2\Omega_n^2} \right) + 2t\cos\theta_n|\alpha_n||\alpha_{n+1}| - \frac{\hbar}{2}\Omega_n \right]. \tag{20}$$

In the Nambu basis $\mathcal{A}^\dagger = (a_1^\dagger, a_2^\dagger, a_3^\dagger, a_1, a_2, a_3)$, we can rewrite this effective Hamiltonian as $H_{sp} = \mathcal{A}^\dagger \mathcal{H}_{sp} \mathcal{A} + E$ with

$$\mathcal{H}_{sp} = \frac{\hbar\omega}{2} \begin{pmatrix} 1-\lambda_1^+ & t'\mathrm{e}^{i\theta_1} & t'\mathrm{e}^{-i\theta_3} & \lambda_1^- & 0 & 0 \\ t'\mathrm{e}^{-i\theta_1} & 1-\lambda_2^+ & t'\mathrm{e}^{i\theta_2} & 0 & \lambda_2^- & 0 \\ t'\mathrm{e}^{i\theta_3} & t'\mathrm{e}^{-i\theta_2} & 1-\lambda_3^+ & 0 & 0 & \lambda_3^- \\ \lambda_1^- & 0 & 0 & 1-\lambda_1^+ & t'\mathrm{e}^{-i\theta_1} & t'\mathrm{e}^{i\theta_3} \\ 0 & \lambda_2^- & 0 & t'\mathrm{e}^{i\theta_1} & 1-\lambda_2^+ & t'\mathrm{e}^{-i\theta_2} \\ 0 & 0 & \lambda_3^- & t'\mathrm{e}^{-i\theta_3} & t'\mathrm{e}^{i\theta_2} & 1-\lambda_3^+ \end{pmatrix}. \tag{21}$$

Excitation spectra $\xi_{1,2,3}$ of Hamiltonian H_{sp} can be obtained by a Bogoliubov transformation ζ to a new basis $\mathcal{B}^\dagger = (b_1^\dagger, b_2^\dagger, b_3^\dagger, b_1, b_2, b_3)$ such that $\mathcal{B} = \zeta\mathcal{A}$ and

$$H_{sp} = E + \sum_{n=1}^{3} \xi_n (b_n^\dagger b_n + b_n b_n^\dagger) = E_{sp} + \sum_{n=1}^{3} 2\xi_n b_n^\dagger b_n \tag{22}$$

with ground state energy $E_{sp} = E + \sum_{n=1}^{3}\xi_n$. We can arrive at these excitation spectra by numerically diagonalizing $\Sigma\mathcal{H}_{sp}$ with diagonal matrix $\Sigma = \mathrm{diag}\{1,1,1,-1,-1,-1\}$ [50]. By exploiting numerical variation method, the ground states can be solved if the energy E_{sp} is minimized and equation (15) is satisfied at the meantime.

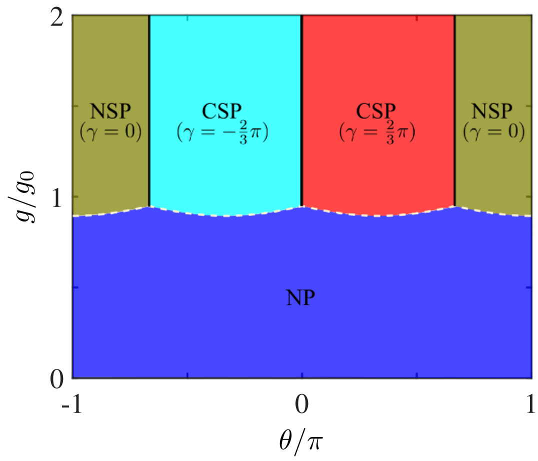

Figure 2. Phase diagram of the aJC triangle model in $g-\theta$ plane. Here 'NP', 'NSP' and 'CSP' are short for 'normal phase', 'normal superradiant phase' and 'chiral superradiant phase'. Black-solid lines represent first-order phase transition and white-dashed line stands for a second-order phase transition. We set other parameters as $\omega = 1$, $\Omega = 10^3\omega$, $t/\hbar = 0.1\omega$ and $\hbar = 1$.

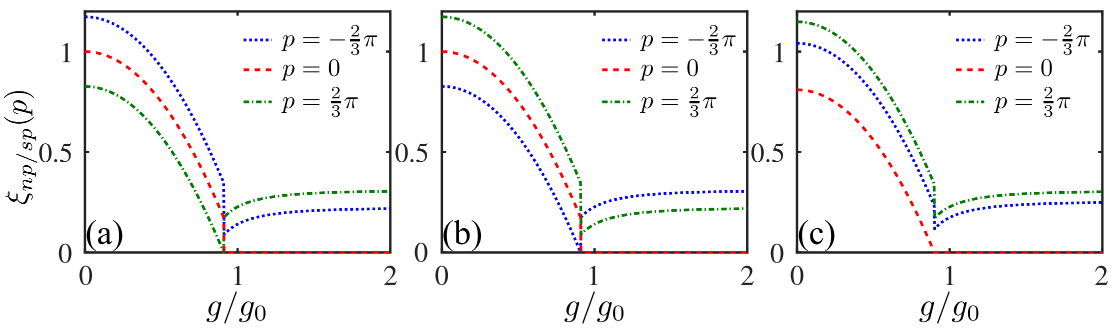

Figure 3. Excitation spectra $\xi_{np/sp}(p)$ of the aJC triangle model varying with on-site coupling strength g. Tunneling phase $\theta = -0.5\pi$ (a), 0.5π (b) and 0.9π (c) respectively. We set other parameters as $\omega = 1$, $\Omega = 10^3\omega$, $t/\hbar = 0.1\omega$ and $\hbar = 1$.

4. Quantum phase transitions and phase diagram

It has been pointed out that QPTs would happen when the on-site interaction increases across some critical value in section 3. In the following we proceed to study effects of symmetries and gauge fields on the ground states. With analytic and numerical variational methods, we figure out a phase diagram for fixed and small enough tunneling t as shown in figure 2. When the on-site coupling g is weak, optical field prefers to stay in a NP, which actually is a vacuum; otherwise, its ground states evolve into superradiant phases with translation symmetry, that is, $|\alpha_n| = \alpha$ and $\gamma_{n+1} - \gamma_n = \gamma$ are not dependent on n. Three types of superradiant phases with infinite degeneracy are induced by the tunneling phase θ, which can make $\gamma = 0$ or $\gamma = \pm\frac{2}{3}\pi$.

If the on-site interaction g is weak, effective Hamiltonian of optical field now is H_{np} (see equation (5) or (7)). In the limit $\Omega/\omega \to \infty$, its ground state is a NP with rescaled energy

$$\mathcal{E}_{np} = \frac{\omega}{\Omega}E_{np} = -\frac{3}{2}\hbar\omega\left(1 + 2\frac{\omega}{\Omega}\frac{g^2}{g_0^2}\right) = -\frac{3}{2}\hbar\omega \tag{23}$$

and rescaled order parameter

$$\sqrt{\frac{\omega}{\Omega}}|\langle a_n\rangle| = \sqrt{\frac{\omega}{\Omega}}|\langle\psi|a_n|\psi\rangle_{np}| = 0. \tag{24}$$

Phase transitions from NP to SPs occur when the energy gap $\xi_{np}(p)|_{\min}$ closes. From the varying characteristics of excitation spectra $\{\xi_{np}(p)\}$ shown in figure 3 , we can know that $\xi_{np}(p)|_{\min} = 0$ can enable us to judge this boundary

$$g_c = g_0\sqrt{1+2t'\cos(\theta-p)}|_{\min} = g_0\sqrt{1+2t'\cos(\theta+\gamma)} = g_0\sqrt{f} \tag{25}$$

with $f(\theta,\gamma) = 1 + 2t'\cos(\theta+\gamma)$. By the aid of this equation, we can determine the boundaries between NP and SPs marked by a white-dashed line in the phase diagram (see figure 2).

If the on-site interaction g is strong enough, effective Hamiltonian of optical field now changes into H_{sp} (see equation (19) or (22)). Its ground states can not be worked out at a glance. It is worth stressing that local translations $\{\alpha_n\}$ should not only minimize the ground energy E_{sp} but also satisfy the preconditions in equation (15). So we can find them out numerically by adapting variational methods, and learn that the translations $\{\alpha_n\}$ should meet that

$$\gamma_{n+1} - \gamma_n = \gamma,\ |\alpha_n| = \alpha = \frac{g}{2g_0}\sqrt{\frac{\Omega}{\omega}}\sqrt{\frac{1}{f^2} - \frac{g_0^4}{g^4}}. \tag{26}$$

Thus, effective Hamiltonian H_{sp} of the optical field turns into

$$H_{sp} = \sum_{n=1}^{3}\hbar\omega\left[\frac{1}{2}[\lambda - 2t'\cos(\theta+\gamma)](a_n^\dagger a_n + a_n a_n^\dagger) + \frac{1}{2}\lambda(a_n^{\dagger 2} + a_n^2) + t'(e^{i\theta_n}a_n^\dagger a_{n+1} + \text{h.c.})\right] + E \tag{27}$$

with $\lambda = \frac{1}{2}f(\theta,\gamma)[1 - \frac{g_0^4}{g^4}f^2(\theta,\gamma)]$, which is translation invariant and also would be reasonable as to a strong and isotopic on-site interaction g. Using firstly a Fourier transformation to the momentum space and then a Bogoliubov transformation to a new basis b_p with $[b_{p_1}, b_{p_2}^\dagger] = \delta_{p_1,p_2}$, Hamiltonian H_{sp} can be diagonalized as (more details can be found in appendix B)

$$H_{sp} = \sum_{p\neq 0}\xi_{sp}(p)\,b_p^\dagger b_p + \lambda\hbar\omega x_0^2 + E_{sp} \tag{28}$$

with energy $E_{sp} = -\frac{3}{4}\hbar\Omega(\frac{g^2}{g_0^2 f} + \frac{g_0^2 f}{g^2}) - \frac{3}{2}\hbar\omega\left[1 + \frac{g_0^2 f^2}{g^2} - \sqrt{(f-1)[f-1-\frac{2}{3}f(1-\frac{g_0^4 f^2}{g^4})]}\right]$. Here we have defined operator $x_0 = (a_0 + a_0^\dagger)/\sqrt{2}$, whose eigenvalues are continuous and belong to $(-\infty, +\infty)$. So the excitation spectra of H_{sp} are

$$\xi_{sp}(p) = \begin{cases} 0 & \text{for}\, p = 0 \\ \frac{\hbar\omega}{2}\left[\sqrt{[\epsilon(p)+\epsilon(-p)]^2 - 4\lambda^2} + \epsilon(p) - \epsilon(-p)\right] & \text{for}\, p\neq 0 \end{cases}. \tag{29}$$

Definition of single-particle energy $\epsilon(p)$ can be found in equation (B.5). Varying of the excitations along with on-site coupling g and tunneling phase θ are plotted in figure 3. Therefore, for the phase transitions from NP to SPs, the energy gap closes and does not reopen anymore. The NP is gapped and the SPs are gapless guaranteed by breaking of the continuous $U(1)$ symmetry, which makes these SPs infinitely degenerate. In the original frame, its corresponding ground state is

$$|\psi\rangle_{sp} = DUU_2|0\rangle_{bp}|-\rangle_\sigma,\ |0\rangle_{bp} = |0\rangle_x|0\rangle_p \tag{30}$$

with $b_p|0\rangle_p = 0$ and $x_0|0\rangle_x = 0$ [51]. From equations (9), (11), (17) and (26), we know that this ground state $|\psi\rangle_{sp}$ is determined by the atom-field interaction g, hopping strength t and phase θ. In the limit $\Omega/\omega\to\infty$, its rescaled ground state energy is

$$\mathcal{E}_{sp} = \frac{\omega}{\Omega}E_{sp} = -\frac{3}{4}\hbar\omega\left(\frac{g^2}{g_0^2 f} + \frac{g_0^2 f}{g^2}\right) \tag{31}$$

and its rescaled order parameter can be calculated as

$$\sqrt{\frac{\omega}{\Omega}}|\langle a_n\rangle| = \sqrt{\frac{\omega}{\Omega}}|\langle\psi|a_n|\psi\rangle_{\text{sp}}| = \sqrt{\frac{\omega}{\Omega}}|\alpha_n| = \sqrt{\frac{\omega}{\Omega}}\alpha = \frac{g}{2g_0}\sqrt{\frac{1}{f^2} - \frac{g_0^4}{g^4}}. \tag{32}$$

In figure 4, we illustrate that this order parameter will continuously increase from zero in NP to non-zero in SPs. Hence, phase transitions from NP to SPs are of second order, which can also be confirmed from discontinuous second-order derivative of the excitation energy with respect to on-site coupling strength g, i.e.

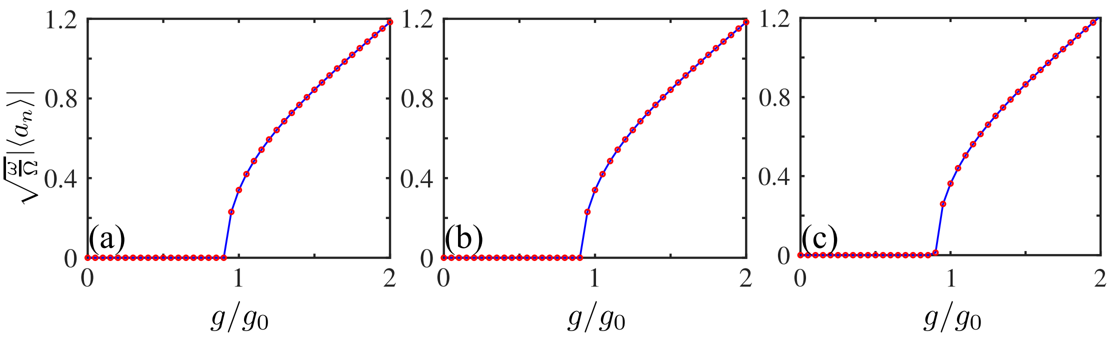

Figure 4. Rescaled order parameter $\sqrt{\frac{\omega}{\Omega}}|\langle a_n\rangle|$ in transition from NP to SP varying with on-site coupling g. Blue lines are its values in the limit of $\Omega/\omega \to \infty$ and red lines stand for that obtained by numerical variation method. The three panels correspond to results with tunneling phase $\theta = -0.5\pi$ (a), 0.5π (b) and 0.9π (c) respectively. We set other parameters as $\omega = 1$, $\Omega = 10^3\omega$, $t/\hbar = 0.1\omega$ and $\hbar = 1$.

$$\partial_g\mathcal{E}_{np} = \partial_g\mathcal{E}_{sp}|_{g=g_c} = 0,\ \partial_g^2\mathcal{E}_{\rm np} = 0,\ \partial_g^2\mathcal{E}_{\rm sp}|_{g=g_c} = -\frac{6\hbar\omega}{g_c^2} \neq 0. \tag{33}$$

At the phase boundaries of NSP and CSP, their corresponding ground energies should be equal

$$\mathcal{E}_{sp}(\theta_c, \gamma = 0) = \mathcal{E}_{sp}\left(\theta_c, \gamma = \pm\frac{2}{3}\pi\right), \tag{34}$$

form which we can acquire that $\theta_c = \pm\frac{2}{3}\pi$ [see the black-solid lines in phase diagram]. Similarly, phase boundary between the two CSPs can be ascertained by solving equation

$$\mathcal{E}_{sp}\left(\theta_c, \gamma = -\frac{2}{3}\pi\right) = \mathcal{E}_{sp}\left(\theta_c, \gamma = \frac{2}{3}\pi\right), \tag{35}$$

which leads to $\theta_c = 0$ (see the black-solid line in phase diagram). To discriminate these diverse SPs, it would be useful to define following current operator [39, 40]

$$I = i\left[\left(a_1^\dagger a_2 + a_2^\dagger a_3 + a_3^\dagger a_1\right) - \text{h.c.}\right]. \tag{36}$$

Its rescaled mean value is

$$\frac{\omega}{\Omega}\langle I\rangle = \frac{\omega}{\Omega}\langle\psi|I|\psi\rangle_{sp} = -6\frac{\omega}{\Omega}\alpha^2\sin(\gamma) = -\frac{3}{2}\frac{g^2}{g_0^2}\left(\frac{1}{f^2} - \frac{g_0^4}{g^4}\right)\sin(\gamma), \tag{37}$$

which reveals that there is no photon current in the NSP, because $\gamma = 0$. We thus name it as normal supreradiant phase. It can be realized that this mean value $\langle I\rangle$ is also zero in the NP, because it is actually a vacuum state of the cavity field. Since $\frac{1}{f^2} - \frac{g_0^4}{g^4} > 0$ in these SPs, direction of photon current $\langle I\rangle$ is dependent on the sign of $\sin(\gamma)$. When $\gamma = \frac{2}{3}\pi$, we know $\langle I\rangle < 0$ and $\frac{\omega}{\Omega}\langle I\rangle = -\frac{3\sqrt{3}}{4}\frac{g^2}{g_0^2}[\frac{1}{(1-t')^2} - \frac{g_0^4}{g^4}]$ at the phase boundaries $\theta_c = 0, \frac{2}{3}\pi$; When $\gamma = -\frac{2}{3}\pi$, we have $\langle I\rangle > 0$ and $\frac{\omega}{\Omega}\langle I\rangle = \frac{3\sqrt{3}}{4}\frac{g^2}{g_0^2}[\frac{1}{(1-t')^2} - \frac{g_0^4}{g^4}]$ at the phase boundaries $\theta_c = 0, -\frac{2}{3}\pi$. Such direction-dependent (chiral) characteristic of the photon current is exhibited in figure 5. Accordingly, transitions between the SPs are all of first order. The NSP only breaks the continuous $U(1)$ symmetry, so its corresponding gapless excitations are normal Goldstone modes. In CSPs, the photon currents are unidirectional (flowing clockwise or anti-clockwise), thus they also break the chiral symmetry and the gapless excitations are chiral Goldstone modes.

5. Detection of superradiant phases

As aJC-type interaction can be easily realized in trapped-ion systems, we consider detection of NSP and CSPs of the aJC triangle model in a trap-ion platform, where a phase transition from NP to SP in the Rabi model has been observed by detecting the spin population and average phonon number [36]. To discriminate NSP

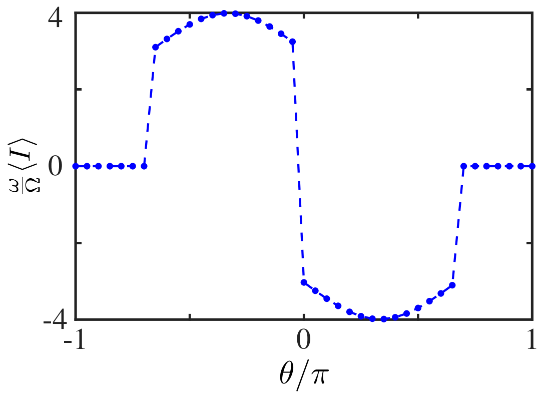

Figure 5. Rescaled photon current $\frac{\omega}{\Omega}\langle I\rangle$ in SPs varying with tunneling phase θ in case of $g = 1.5g_0$. We set other parameters as $\omega = 1$, $\Omega = 10^3\omega$, $t/\hbar = 0.1\omega$ and $\hbar = 1$.

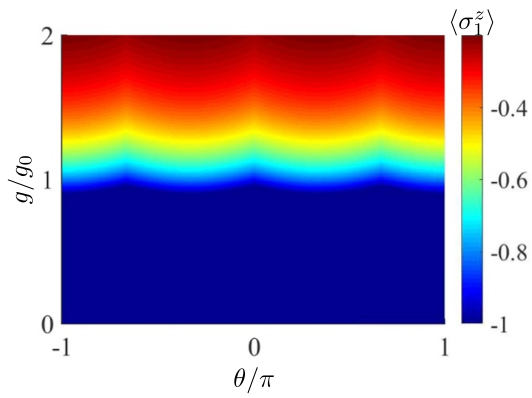

Figure 6. Mean value $\langle\sigma_1^z\rangle$ of the ground states in $g-\theta$ plane. We set other parameters as $\omega = 1$, $\Omega = 10^3\omega$, $t/\hbar = 0.1\omega$ and $\hbar = 1$.

and CSPs in the phase diagram (see figure 2), the point is to measure phase γ of the complex translation α_n, which can be probed by measuring spin of the '$n = 1$' trapped ion. In the frequency limit $\Omega/\omega \to \infty$, we know that $\langle\sigma_1^z\rangle = -1$ in NP and $\langle\sigma_1^z\rangle = -\Omega/\sqrt{\Omega^2 + g^2\alpha^2} \neq -1$ in SPs as shown in figure 6. As a result, we can acquire the value of α by probing σ_1^z in an experiment. After observing a non-zero α, we can infer the phase γ by utilizing equation (26), then determine the SPs.

We can also verify the SPs by probing the blue sideband transitions of the '$n = 1$' trapped ion, which consists of three steps (more details can be found in appendix C):

(i) applying a short optical pumping pulse to pump internal state of the '$n = 1$' trapped ion into $|g\rangle_1$. This pulse should be set short enough so that its effect on the motional state (phonon state) population of the three trapped ions can be neglected. In the frequency limit $\Omega/\omega \to \infty$, we can prepare the system into an initial state $|\psi(0)\rangle$ (see equation (C.2));

(ii) a running wave light field is used to drive blue sideband transition of the '$n = 1$' trapped ion for various time intervals $\tilde{t}$. Under the resonance condition of first blue sideband [52], its evolution is described by the interaction Hamiltonian $H_i = \frac{\hbar\Gamma}{2}(a_1^\dagger\sigma_1^\dagger + a_1\sigma_1^-)$ with coupling frequency Γ determined by the external light field. At time $\tilde{t}$, wave function of the system evolves into $|\psi(\tilde{t})\rangle = \mathrm{e}^{-\frac{i}{\hbar}H_i\tilde{t}}|\psi(0)\rangle$.

(iii) measuring the probability to find the '$n = 1$' trapped ion in its ground state $|g\rangle_1$, which can be defined as $P_g(\tilde{t}) = \langle\psi(\tilde{t})|(|g\rangle_1\langle g|)|\psi(\tilde{t})\rangle$. Through meticulous analysis, we can derive that

$$P_g(\tilde{t}) = \frac{1}{2}\left(1 + \cos\left(\tilde{\Gamma}\tilde{t}\right) + \sum_n \frac{H_n^2(0)}{2^n n!\sqrt{\pi}}\cos\left(\tilde{\Gamma}_n\tilde{t}\right) + \cdots\right), \tag{38}$$

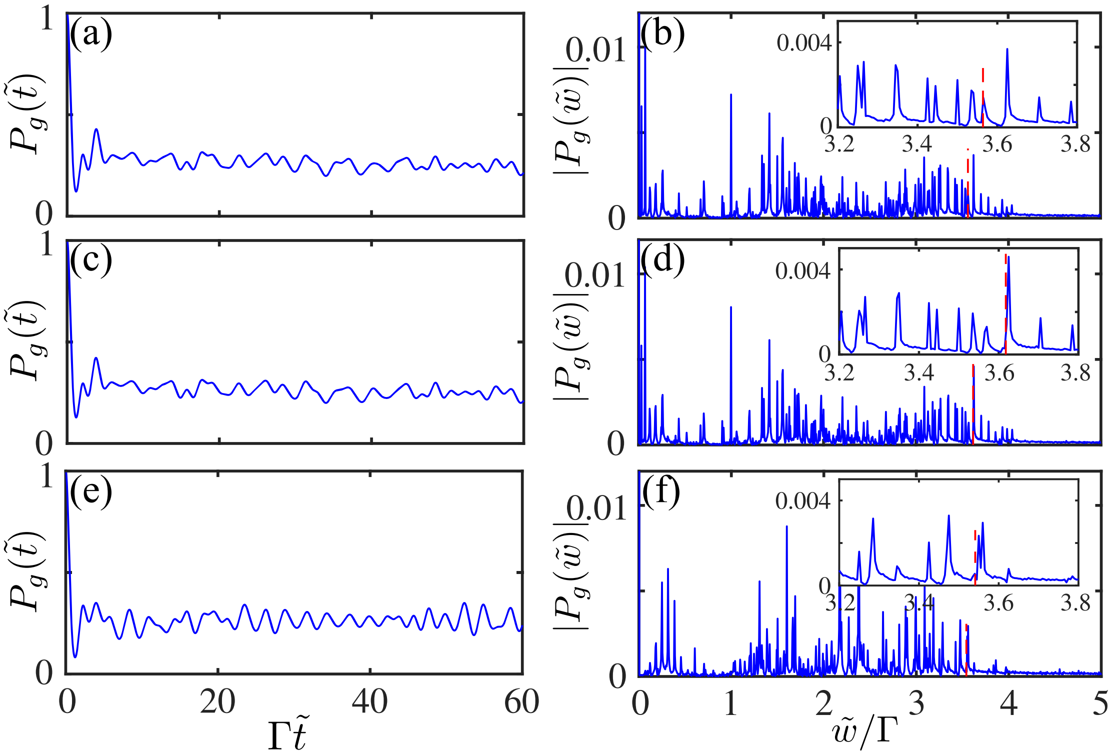

Figure 7. Probability $P_g(\tilde{t})$ and its Fourier transformation $P_g(\tilde{w})$ in cases of $\theta = -0.3\pi$ ((a) and (b)), $\theta = -0.5\pi$ ((c) and (d)), $\theta = 0.8\pi$ ((e) and (f)). Red-dash lines in figures (b/d/f) are the line of $\tilde{w} = \tilde{\Gamma}$. We set other parameters as $\omega = 1$, $\Omega = 10^3\omega$, $t/\hbar = 0.1\omega$, $g = 1.01g_c$, $\Gamma = 20\omega$ and $\hbar = 1$.

where $\tilde{\Gamma} = \sqrt{\alpha^2 + \frac{2}{3}\mu^2}\Gamma$, $\tilde{\Gamma}_n = \sqrt{\frac{n+1}{3}}\Gamma$, $H_n(x)$ is the Hermitian polynomials and μ is defined in equation (B.6). Although there are many undetermined oscillation frequencies in the probability $P_g(\tilde{t})$, we can extract analytically two types of oscillation frequencies $\tilde{\Gamma}_n$ and $\tilde{\Gamma}$. Just as expected, the frequencies $\tilde{\Gamma}_n$ are closely related to populations of Fock states $|n\rangle$ in the ground state $|0\rangle_x$ [52]. The frequency $\tilde{\Gamma}$ originates from the complex translation (α_n) and excitations (μ), which can give us information about γ and α.

Following the procedures provided above, we numerically calculate the spin evolution probability $P_g(\tilde{t})$ of the '$n = 1$' trapped ion and its Fourier transformation $P_g(\tilde{w}) = \int P_g(\tilde{t})e^{-i\tilde{w}\tilde{t}}d\tilde{t}$ as shown in figure 7. It is clear that oscillation of the spin probability $P_g(\tilde{t})$ turns out to be very intricate after evolution of long enough time in both CSPs (figures 7(a) and (c)) and NSP (figure 7(e)), which implies that abundant oscillation frequencies exist in the spin evolution probability $P_g(\tilde{t})$ (see figures 7(b), (d) and (f)). The subplots in figures 7(b), (d) and (f) explicitly display that a summit of the probability amplitude $|P_g(\tilde{w})|$ arises at a frequency near the predicted value $\tilde{w} = \tilde{\Gamma} = \sqrt{\alpha^2 + \frac{2}{3}\mu^2}\Gamma$ (the red-dash lines). Consequently, once this kind of summit is found in realistic evolution experiments, we can assert that the aJC triangle model is in a superradiant phase, and then identify the SP is NSP or CSP. It should be emphasized that the coupling frequency Γ should be set large enough such that the evolution time needed can be much less than the system's decoherence time.

6. Conclusion

In this paper, we have studied QPTs of the aJC triangle model in the infinite frequency limit by analytical and numerical variation methods. The on-site atom-cavity coupling gives rise to a continuous phase transition from a gapped NP to a gapless superradiant phase breaking the continuous $U(1)$ symmetry. Meantime, the external artificial gauge field can lead to first-order phase transitions between NSP and CSPs. These SPs are of infinite degeneracy. There exist two types of directed photon currents in the CSPs, which therefore also break the chiral symmetry. Combined interaction of the atom-cavity coupling and artificial gauge fields can yield novel quantum states in the aJC triangle model. Distinguishing of NSP and CSPs can be fulfilled by utilizing the suggested detection scheme that is intended to seek out the phase γ and special oscillation frequency $\tilde{\Gamma}$ of the spin evolution probability $P_g(\tilde{t})$. Our study may advance the search for exotic quantum states in few-body systems and their applications in quantum simulation or quantum metrology.

Data availability statement

All data that support the findings of this study are included within the article (and any supplementary files).

Acknowledgments

This work was funded National Natural Science Foundation of China (Grant Nos. 12104363, 11974334 and 11774332). X F Z and Z W Z acknowledge the support from Innovation Program for Quantum Science and Technology 360 (Grant No. 2021ZD0301200). Y C Z acknowledges the support of National Natural Science Foundation of China (Grant No. 12104359), the National Key R & D Program of China (2021YFA1401700), Shaanxi Academy of Fundamental Sciences (Mathematics, Physics) (Grant No. 22JSY036), Open project of Low Dimensional Quantum Physics State Key Laboratory (Grant No. KF202104), Xi'an Jiaotong University through the 'Young Top Talents Support Plan' and Basic Research Funding (Grant No. xtr042021012).

Appendix A. Deriving effective Hamiltonian of the optical field

In this section, we show a detailed derivation of the effective Hamiltonian in weak and strong on-site atomic-cavity coupling. We rewrite the Hamiltonian in equation (1) as

$$H = \sum_{n=1}^{3} [H_n + H_{nn'}] \tag{A.1}$$

with

$$H_n = \frac{\hbar\Omega}{2}\sigma_n^z + \hbar\omega a_n^\dagger a_n + \frac{\hbar g}{2}\left(a_n^\dagger \sigma_n^\dagger + a_n \sigma_n^-\right), \tag{A.2}$$

$$H_{nn'} = \left(te^{i\theta} a_n^\dagger a_{n+1} + \text{h.c.}\right). \tag{A.3}$$

Here H_n is the intra-cavity part and depicts interaction between a photon and an atom in the nth cavity, while $H_{nn'}$ is the tunneling Hamiltonian of a photon between adjacent cavities. Apparently, we have these commutation relationships in hand

$$\left[a_n, a_{n'}^\dagger\right] = \delta_{n,n'}, \left[\sigma_n^+, \sigma_{n'}^-\right] = \sigma_n^z \delta_{n,n'}, \left[\sigma_n^z, \sigma_{n'}^\pm\right] = \pm 2\sigma_n^\pm \delta_{n,n'}. \tag{A.4}$$

First, for weak on-site coupling g, we should make a Schrieffer–Wolff transformation

$$U_1 = \mathrm{e}^{-S_1} \text{ with } S_1 = \frac{g}{2(\Omega + \omega)} \sum_{n=1}^{3} \left(a_n^\dagger \sigma_n^\dagger - a_n \sigma_n^-\right). \tag{A.5}$$

Under this unitary transformation, we can obtain a new Hamiltonian

$$H_1 = U_1^\dagger H U_1 = \sum_{n=1}^{3} \left[U_1^\dagger H_n U_1 + U_1^\dagger H_{nn'} U_1)\right]. \tag{A.6}$$

Using relationships in equation (A.4), it is easy to acquire that

$$
\begin{aligned}
U_1^\dagger H_n U_1 &= \frac{\hbar}{2}\Omega\sigma_n^z + \hbar\omega a_n^\dagger a_n + \frac{\hbar g^2}{8\Omega}\frac{1}{1+\omega/\Omega}[(2a_n^\dagger a_n+1)\sigma_n^z - 1] + O(g^3) \\
&= \frac{\hbar}{2}\Omega\sigma_n^z + \hbar\omega a_n^\dagger a_n + \hbar\omega\frac{g^2}{2g_0^2}[(2a_n^\dagger a_n+1)\sigma_n^z - 1] + O(g^3), \\
U_1^\dagger H_{nn'} U_1 &= t\mathrm{e}^{i\theta}\Big[a_n^\dagger a_{n+1} - \frac{g}{2\Omega}\frac{1}{1+\omega/\Omega}(a_n^\dagger\sigma_{n+1}^\dagger + a_{n+1}\sigma_n^-) + \frac{g^2}{4\Omega^2}\frac{1}{(1+\omega/\Omega)^2}\sigma_n^-\sigma_{n+1}^\dagger \\
&\quad - \frac{g^2}{8\Omega^2}\frac{1}{(1+\omega/\Omega)^2}(a_n^\dagger a_{n+1}\sigma_{n+1}^z + a_n^\dagger a_{n+1}\sigma_n^z)\Big] + \text{h.c.} + O(g^3) \\
&= t\mathrm{e}^{i\theta}\Big[a_n^\dagger a_{n+1} - \frac{g}{g_0}\sqrt{\frac{\omega}{\Omega}}(a_n^\dagger\sigma_{n+1}^\dagger + a_{n+1}\sigma_n^-) + \frac{g^2}{g_0^2}\frac{\omega}{\Omega}\sigma_n^-\sigma_{n+1}^\dagger \\
&\quad - \frac{g^2}{2g_0^2}\frac{\omega}{\Omega}(a_n^\dagger a_{n+1}\sigma_{n+1}^z + a_n^\dagger a_{n+1}\sigma_n^z)\Big] + \text{h.c.} + O(g^3) \\
&= t(\mathrm{e}^{i\theta}a_n^\dagger a_{n+1} + \mathrm{e}^{-i\theta}a_{n+1}^\dagger a_n) + O(g^3)
\end{aligned}
$$

in the frequency limit $\Omega/\omega \to \infty$. Here we have defined a finite parameter $g_0 = 2\sqrt{\Omega\omega}$. Thus, to second order of g, this Hamiltonian becomes

$$
\begin{aligned}
H_1 &\approx \sum_{n=1}^{3}\Big[\frac{\hbar}{2}\Omega\sigma_n^z + \hbar\omega a_n^\dagger a_n + \hbar\omega\frac{g^2}{2g_0^2}[(2a_n^\dagger a_n+1)\sigma_n^z - 1] + t(\mathrm{e}^{i\theta}a_n^\dagger a_{n+1} + \text{h.c.})\Big] \\
&= \sum_{n=1}^{3}\Big[\frac{\hbar}{2}\Omega\sigma_n^z + \hbar\omega(1+\frac{g^2}{g_0^2}\sigma_n^z)a_n^\dagger a_n + \frac{\hbar\omega}{2}\frac{g^2}{g_0^2}(\sigma_n^z - 1) \\
&\quad + t(\mathrm{e}^{i\theta}a_n^\dagger a_{n+1} + \mathrm{e}^{-i\theta}a_{n+1}^\dagger a_n)\Big].
\end{aligned} \tag{A.7}
$$

As transition frequency Ω of the two-level atom is dominated, atoms should stay at their ground states $|0\rangle_\sigma = \prod_{n=1}^{3}|g\rangle_n$. Then, physical behaviors of the optical field are governed by Hamiltonian $H_{np} = \langle 0|H_1|0\rangle_\sigma$, whose concrete form becomes

$$
H_{np} = -\frac{3}{2}\hbar\left(\Omega + 2\omega\frac{g^2}{g_0^2}\right) + \sum_{n=1}^{3}\left[\hbar\omega\left(1-\frac{g^2}{g_0^2}\right)a_n^\dagger a_n + t\left(\mathrm{e}^{i\theta}a_n^\dagger a_{n+1} + \text{h.c.}\right)\right]. \tag{A.8}
$$

At strong on-site coupling g, the optical field can no longer remain in a vacuum state. We need to make a local translation to the cavity field

$$
D = \exp\left[\sum_{n=1}^{3}\left(\alpha_n a_n^\dagger - \alpha_n^* a_n\right)\right] \tag{A.9}
$$

with $\alpha_n = |\alpha_n|\mathrm{e}^{i\gamma_n}$, and get a translated Hamiltonian $H_2' = D^\dagger H D$. Then this new Hamiltonian H_2' reads

$$
\begin{aligned}
H_2' &= \sum_{n=1}^{3}\Big[\frac{\hbar}{2}\Omega\sigma_n^z + \hbar\omega a_n^\dagger a_n + \frac{\hbar g}{2}(a_n^\dagger\sigma_n^\dagger + a_n\sigma_n^-) + t(\mathrm{e}^{i\theta}a_n^\dagger a_{n+1} + \text{h.c.}) \\
&\quad + \hbar\omega(\alpha_n a_n^\dagger + \alpha_n^* a_n + |\alpha_n|^2) + \frac{\hbar g}{2}(\alpha_n^*\sigma_n^\dagger + \alpha_n\sigma_n^-) \\
&\quad + t\Big[\mathrm{e}^{i\theta}(\alpha_{n+1}a_n^\dagger + \alpha_n^* a_{n+1} + \alpha_n^*\alpha_{n+1}) + \text{h.c.}\Big]\Big] \\
&= \sum_{n=1}^{3}\Big[\frac{\hbar}{2}\Omega\sigma_n^z + \hbar\omega a_n^\dagger a_n + \frac{\hbar g}{2}(a_n^\dagger\sigma_n^\dagger + a_n\sigma_n^-) + t(\mathrm{e}^{i\theta}a_n^\dagger a_{n+1} + \text{h.c.}) \\
&\quad + \frac{\hbar g}{2}(\alpha_n^*\sigma_n^\dagger + \alpha_n\sigma_n^-) + [(\hbar\omega\alpha_n + t\mathrm{e}^{i\theta}\alpha_{n+1} + t\mathrm{e}^{-i\theta}\alpha_{n-1})a_n^\dagger + \text{h.c.}] \\
&\quad + (\hbar\omega|\alpha_n|^2 + t\mathrm{e}^{i\theta}\alpha_n^*\alpha_{n+1} + t\mathrm{e}^{-i\theta}\alpha_{n+1}^*\alpha_n)\Big].
\end{aligned} \tag{A.10}
$$

To clarify effects of the local translation α_n, it can be helpful to apply a unitary transformation

$$
U = \exp\left[i\sum_{n=1}^{3}\gamma_n\left(a_n^\dagger a_n - \sigma_n^\dagger\sigma_n^-\right)\right]. \tag{A.11}
$$

Because it can be identified that

$$U^\dagger \sigma_n^z U = \sigma_n^z,\ U^\dagger \sigma_n^\dagger U = \mathrm{e}^{i\gamma_n}\sigma_n^\dagger, U^\dagger a_n^\dagger U = \mathrm{e}^{-i\gamma_n} a_n^\dagger,$$

we will get a new translated Hamiltonian $\mathcal{H}_2' = U^\dagger H' U$ and know that

$$\begin{aligned}\mathcal{H}_2' = \sum_{n=1}^{3} \Big[& H_{qn} + \hbar\omega a_n^\dagger a_n + \frac{\hbar g}{2}(a_n^\dagger \sigma_n^\dagger + a_n \sigma_n^-) + t(\mathrm{e}^{i\theta_n} a_n^\dagger a_{n+1} + \mathrm{h.c.}) \\ & + [(\hbar\omega|\alpha_n| + t\mathrm{e}^{i\theta_n}|\alpha_{n+1}| + t\mathrm{e}^{-i\theta_{n-1}}|\alpha_{n-1}|)a_n^\dagger + \mathrm{h.c.}] \\ & + (\hbar\omega|\alpha_n|^2 + 2t\cos\theta_n|\alpha_n||\alpha_{n+1}|)\Big] \end{aligned} \tag{A.12}$$

with phase $\theta_n = \theta + \gamma_{n+1} - \gamma_n$ and a local atom Hamiltonian

$$H_{qn} = \frac{\hbar}{2}\Omega\sigma_n^z + \frac{\hbar g}{2}|\alpha_n|\sigma_n^x. \tag{A.13}$$

From equation (A.12), we can realize that if there are photons in cavities, on one hand, they may induce an effective tunneling phase θ_n; on the other hand, they can perturb an atom in the nth cavity away from its ground state $|g\rangle_n$. As to this two-level atom, its Hamiltonian H_{qn} can be diagonalized as

$$H_{qn} = \frac{\hbar}{2}\Omega_n\tau_n^z,\ \Omega_n = \sqrt{\Omega^2 + g^2|\alpha_n|^2} \tag{A.14}$$

with eigenstates

$$|+\rangle_n = \cos(\beta_n)|e\rangle_n + \sin(\beta_n)|g\rangle_n, |-\rangle_n = \sin(\beta_n)|e\rangle_n - \cos(\beta_n)|g\rangle_n \tag{A.15}$$

and $\sin(\beta_n) = \sqrt{\frac{1}{2}(1 - \frac{\Omega}{\Omega_n})}$, $\cos(\beta_n) = \sqrt{\frac{1}{2}(1 + \frac{\Omega}{\Omega_n})}$, $\tau_n^z = |+\rangle_n\langle+| - |-\rangle_n\langle-|$. In this eigenstates bases, we can have that

$$\begin{aligned}\sigma_n^\dagger = (\sigma_n^-)^\dagger &= \frac{1}{2}\sin(2\beta_n)\tau_n^z - \cos^2(\beta_n)\tau_n^\dagger + \sin^2(\beta_n)\tau_n^- \\ &= \frac{1}{2}\left[\frac{g|\alpha_n|}{\Omega_n}\tau_n^z - \left(1 + \frac{\Omega}{\Omega_n}\right)\tau_n^\dagger + \left(1 - \frac{\Omega}{\Omega_n}\right)\tau_n^-\right]\end{aligned} \tag{A.16}$$

with $\tau_n^\dagger = (\tau_n^-)^\dagger = |+\rangle_n\langle-|$. And Hamiltonian $\mathcal{H}_2'$ can be changed into

$$\begin{aligned}\mathcal{H}_2' = \sum_{n=1}^{3} \Bigg[& \left(\left[\left(\frac{\hbar g^2}{4\Omega_n}\tau_n^z + \hbar\omega\right)|\alpha_n| + t\mathrm{e}^{i\theta_n}|\alpha_{n+1}| + t\mathrm{e}^{-i\theta_{n-1}}|\alpha_{n-1}|\right] a_n^\dagger + \mathrm{h.c.}\right) \\ & - \frac{\hbar g}{4}\left[(1 + \frac{\Omega}{\Omega_n})(a_n^\dagger\tau_n^\dagger + a_n\tau_n^-) - (1 - \frac{\Omega}{\Omega_n})(a_n^\dagger\tau_n^- + a_n\tau_n^\dagger)\right] \\ & + \frac{\hbar}{2}\Omega_n\tau_n^z + \hbar\omega a_n^\dagger a_n + t(\mathrm{e}^{i\theta_n}a_n^\dagger a_{n+1} + \mathrm{h.c.}) \\ & + (\hbar\omega|\alpha_n|^2 + 2t\cos\theta_n|\alpha_n||\alpha_{n+1}|)\Bigg].\end{aligned} \tag{A.17}$$

As atomic energy $\hbar\Omega_n$ is predominant in Hamiltonian $\mathcal{H}_2'$, it is valid to assume that the atom in each cavity would keep in its ground state $|-\rangle_n$. The first line in equation (A.17) can be eliminated by demanding that

$$\left(\hbar\omega - \frac{\hbar g^2}{4\Omega_n}\right)|\alpha_n| + t\mathrm{e}^{i\theta_n}|\alpha_{n+1}| + t\mathrm{e}^{-i\theta_{n-1}}|\alpha_{n-1}| = 0, \tag{A.18}$$

which is equal to

$$|\alpha_{n+1}|\sin\theta_n - |\alpha_{n-1}|\sin\theta_{n-1} = 0, \tag{A.19}$$

$$\left(\hbar\omega - \frac{\hbar g^2}{4\Omega_n}\right)|\alpha_n| + t(|\alpha_{n+1}|\cos\theta_n + |\alpha_{n-1}|\cos\theta_n) = 0 \tag{A.20}$$

with $n = 1,2,3$. Under this situation, Hamiltonian $\mathcal{H}_2'$ becomes

$$\mathcal{H}_2' = \sum_{n=1}^{3}\Bigg[\frac{\hbar g}{4}\left[\left(1-\frac{\Omega}{\Omega_n}\right)(a_n^\dagger\tau_n^- + a_n\tau_n^\dagger) - \left(1+\frac{\Omega}{\Omega_n}\right)(a_n^\dagger\tau_n^\dagger + a_n\tau_n^-)\right] + \frac{\hbar}{2}\Omega_n\tau_n^z + \hbar\omega a_n^\dagger a_n + t(\mathrm{e}^{i\theta_n}a_n^\dagger a_{n+1} + \mathrm{h.c.}) + (\hbar\omega|\alpha_n|^2 + 2t\cos\theta_n|\alpha_n||\alpha_{n+1}|)\Bigg], \tag{A.21}$$

which can be diagonalized by another Schrieffer–Wolff transformation $U_2 = \mathrm{e}^{-S_2}$ with

$$S_2 = \sum_{n=1}^{3}\frac{g}{4}\left[\frac{1-\frac{\Omega}{\Omega_n}}{\Omega_n-\omega}\left(a_n\tau_n^\dagger - a_n^\dagger\tau_n^-\right) - \frac{1+\frac{\Omega}{\Omega_n}}{\Omega_n+\omega}\left(a_n^\dagger\tau_n^\dagger - a_n\tau_n^-\right)\right]. \tag{A.22}$$

We mark the transformed Hamiltonian using H_2 and expand it in this way

$$H_2 = U_2^\dagger\mathcal{H}_2'U_2 = \mathcal{H}_2' + [S_2,\mathcal{H}_2'] + \frac{1}{2!}[S_2,[S_2,\mathcal{H}_2']] + \cdots. \tag{A.23}$$

In the limit of $\Omega/\omega\to\infty$, we can find that

$$[S_2,\mathcal{H}_2'] = \sum_{n=1}^{3}\Bigg[-\frac{\hbar g}{4}\left[\left(1-\frac{\Omega}{\Omega_n}\right)(a_n^\dagger\tau_n^- + a_n\tau_n^\dagger) - \left(1+\frac{\Omega}{\Omega_n}\right)(a_n^\dagger\tau_n^\dagger + a_n\tau_n^-)\right] + \frac{\hbar\omega}{2}\frac{g^2\Omega}{g_0^2\Omega_n}\left[\left(1+\frac{\Omega^2}{\Omega_n^2}\right)(2a_n^\dagger a_n+1)\tau_n^z - \left(1-\frac{\Omega^2}{\Omega_n^2}\right)(a_n^{\dagger 2}+a_n^2)\tau_n^z - \frac{2\Omega}{\Omega_n}\right]\Bigg]$$

and

$$[S_2,[S_2,\mathcal{H}_2']] = \sum_{n=1}^{3}\frac{\hbar\omega}{2}\frac{g^2\Omega}{g_0^2\Omega_n}\left[\left(1-\frac{\Omega^2}{\Omega_n^2}\right)\left(a_n^{\dagger 2}+a_n^2\right)\tau_n^z - \left(1+\frac{\Omega^2}{\Omega_n^2}\right)\left(2a_n^\dagger a_n+1\right)\tau_n^z + \frac{2\Omega}{\Omega_n}\right] + O\left(g^3\right).$$

With the aid of these two equations, Hamiltonian H_2 becomes

$$H_2 \approx \sum_{n=1}^{3}\Bigg[\hbar\omega|\alpha_n|^2 + 2t\cos\theta_n|\alpha_n||\alpha_{n+1}| - \frac{\hbar\omega}{2}\frac{g^2\Omega}{g_0^2\Omega_n} + \frac{\hbar}{2}\Omega_n\tau_n^z + \hbar\omega a_n^\dagger a_n + t(\mathrm{e}^{i\theta_n}a_n^\dagger a_{n+1} + \mathrm{h.c.}) + \frac{\hbar\omega}{4}\frac{g^2\Omega}{g_0^2\Omega_n}\left[(1+\frac{\Omega^2}{\Omega_n^2})(2a_n^\dagger a_n+1)\tau_n^z - (1-\frac{\Omega^2}{\Omega_n^2})(a_n^{\dagger 2}+a_n^2)\tau_n^z\right]\Bigg] \tag{A.24}$$

to second order of on-site coupling g. So Hamiltonian of the cavity field can be defined as $H_{\mathrm{sp}} = \langle -|H_2|-\rangle_\sigma$ with $|-\rangle_\sigma = \prod_{n=1}^{3}|-\rangle_n$, which can be in form of

$$H_{\mathrm{sp}} = \sum_{n=1}^{3}\Bigg[\hbar\omega|\alpha_n|^2 + 2t\cos\theta_n|\alpha_n||\alpha_{n+1}| - \frac{\hbar\omega}{4}\frac{g^2\Omega}{g_0^2\Omega_n}\left(1+\frac{\Omega}{\Omega_n}\right)^2 - \frac{\hbar}{2}\Omega_n + t(\mathrm{e}^{i\theta_n}a_n^\dagger a_{n+1} + \mathrm{h.c.}) + \hbar\omega\left[1-\frac{1}{2}\frac{g^2\Omega}{g_0^2\Omega_n}\left(1+\frac{\Omega^2}{\Omega_n^2}\right)\right]a_n^\dagger a_n + \frac{\hbar\omega}{4}\frac{g^2\Omega}{g_0^2\Omega_n}(1-\frac{\Omega^2}{\Omega_n^2})(a_n^{\dagger 2}+a_n^2)\Bigg]. \tag{A.25}$$

Appendix B. Diagonalizing effective Hamiltonian H_{sp}

In superradiant phases, effective Hamiltonian of optical field is H_{sp} (see equation (19) or (22)). We find that the translations $\{\alpha_n\}$ should meet

$$\gamma_{n+1}-\gamma_n=\gamma,\ |\alpha_n|=\alpha=\frac{g}{2g_0}\sqrt{\frac{\Omega}{\omega}}\sqrt{\frac{1}{f^2}-\frac{g_0^4}{g^4}} \tag{B.1}$$

with $f(\theta,\gamma)=1+2t'\cos(\theta+\gamma)$. Thus, effective Hamiltonian H_{sp} will turn into

$$H_{\rm sp}=\sum_{n=1}^{3}\hbar\omega\left[\frac{1}{2}[\lambda-2t'\cos(\theta+\gamma)](a_n^\dagger a_n+a_na_n^\dagger)+\frac{1}{2}\lambda(a_n^{\dagger 2}+a_n^2)+t'(\mathrm{e}^{i(\theta+\gamma)}a_n^\dagger a_{n+1}+\mathrm{h.c.})\right]+E \tag{B.2}$$

with $\lambda=\frac{1}{2}f(\theta,\gamma)[1-\frac{g_0^4}{g^4}f^2(\theta,\gamma)]$. Because it is translation invariant, we can make a Fourier transformation to the momentum space and will discover that

$$H_{\rm sp}=\sum_{p>0}[2\mathcal{H}(p)-\epsilon(-p)\hbar\omega]+\mathcal{H}(0)-\hbar\omega[3t'\cos(\theta+\gamma)-\lambda]+E. \tag{B.3}$$

Concrete form of Hamiltonian $\mathcal{H}(p)$ is

$$\mathcal{H}(p)=\frac{\hbar\omega}{2}\left[\epsilon(p)a_p^\dagger a_p+\epsilon(-p)a_{-p}a_{-p}^\dagger+\lambda\left(a_p^\dagger a_{-p}^\dagger+a_{-p}a_p\right)\right] \tag{B.4}$$

with single-particle energy

$$\epsilon(p)=\lambda+2t'[\cos(\theta+\gamma-p)-\cos(\theta+\gamma)]. \tag{B.5}$$

Using a Bogoliubov transformation

$$a_p=\mu b_p-\nu b_{-p}^\dagger,\ a_{-p}^\dagger=-\nu b_p+\mu b_{-p}^\dagger \tag{B.6}$$

with $\mu=\frac{1}{\sqrt{2}}[\sqrt{\frac{[\epsilon(p)+\epsilon(-p)]^2}{[\epsilon(p)+\epsilon(-p)]^2-4\lambda^2}}+1]^{1/2}$, $\nu=\frac{1}{\sqrt{2}}[\sqrt{\frac{[\epsilon(p)+\epsilon(-p)]^2}{[\epsilon(p)+\epsilon(-p)]^2-4\lambda^2}}-1]^{1/2}$ and $[b_{p_1},b_{p_2}^\dagger]=\delta_{p_1,p_2}$, Hamiltonian $\mathcal{H}(p)$ can be diagonalized as

$$\mathcal{H}(p)=\xi(p)b_p^\dagger b_p+\xi(-p)b_{-p}^\dagger b_{-p}+\xi(-p) \tag{B.7}$$

with discrete excitation spectra

$$\xi(p)=\frac{\hbar\omega}{4}\left[\sqrt{[\epsilon(p)+\epsilon(-p)]^2-4\lambda^2}+\epsilon(p)-\epsilon(-p)\right]. \tag{B.8}$$

It should be noted that because $\epsilon(0)=\lambda\hbar\omega$, we can not use the same way to diagonalize $\mathcal{H}(0)$ [53], whose concrete form is

$$\mathcal{H}(0)=\frac{1}{2}\lambda\hbar\omega\left(a_0+a_0^\dagger\right)^2=\lambda\hbar\omega x_0^2 \tag{B.9}$$

with $x_0=(a_0+a_0^\dagger)/\sqrt{2}$. Its eigenvalues belong to $(-\infty,+\infty)$, so the spectrum of $\mathcal{H}(0)$ is continuous running from 0 to $+\infty$. The excitation energy is $\xi(p=0)=0$. In this way, we can reach the diagonalized form of Hamiltonian H_{sp}

$$H_{sp}=\sum_{p\neq 0}2\xi(p)b_p^\dagger b_p+\lambda\hbar\omega x_0^2+E_{sp}. \tag{B.10}$$

The ground energy E_{sp} can be calculated as

$$\begin{aligned}E_{sp}&=E+\sum_{p>0}[2\xi(-p)-\epsilon(-p)\hbar\omega]-\hbar\omega[3t'\cos(\theta+\gamma)-\lambda]\\&=-\frac{3}{2}\hbar\omega\left[1+\frac{g_0^2f^2}{g^2}-\sqrt{(f-1)\left[f-1-\frac{2}{3}f\left(1-\frac{g_0^4f^2}{g^4}\right)\right]}\right]\\&\quad-\frac{3}{4}\hbar\Omega\left(\frac{g^2}{g_0^2f}+\frac{g_0^2f}{g^2}\right).\end{aligned} \tag{B.11}$$

Appendix C. Deriving the evolution probability in a blue sideband transition

We try to provide detailed presentations of deriving the evolution probability in a blue sideband transition. Firstly, a short optical pumping pulse is applied to pump the internal state of the '$n=1$' trapped ion into $|g\rangle_1$. This pulse should be set short enough so that its effect on the motional state (phonon state) population of the three trapped ions can be neglected. In a superradiant phase, its state function is $|\psi\rangle_{sp}$ (see equation (30)) in the frequency limit $\Omega/\omega\to\infty$. The concrete form of these unitary operators in $|\psi\rangle_{sp}$ becomes

$$D=\mathrm{e}^{\alpha\sum_{n=1}^{3}\left(\mathrm{e}^{i\gamma}a_n^{\dagger}-\mathrm{e}^{-i\gamma}a_n\right)}=\prod_{n=1}^{3}\tilde{D}_n,\ \tilde{D}_n=\mathrm{e}^{\alpha\left(\mathrm{e}^{i\gamma}a_n^{\dagger}-\mathrm{e}^{-i\gamma}a_n\right)},$$
$$U=\mathrm{e}^{i\gamma\sum_{n=1}^{3}\left(a_n^{\dagger}a_n-\sigma_n^{\dagger}\sigma_n^{-}\right)}=\prod_{n=1}^{3}\tilde{U}_n,\ \tilde{U}_n=\mathrm{e}^{i\gamma\left(a_n^{\dagger}a_n-\sigma_n^{\dagger}\sigma_n^{-}\right)},$$
$$U_2=\mathrm{e}^{-A_-\sum_{n=1}^{3}\left(a_n\tau_n^{\dagger}-a_n^{\dagger}\tau_n^{-}\right)+A_+\sum_{n=1}^{3}\left(a_n^{\dagger}\tau_n^{\dagger}-a_n\tau_n^{-}\right)}$$

with $A_{\pm}=\frac{1}{2}\sqrt{\frac{\omega}{\Omega}}\frac{g_cf}{g}(1\pm\frac{g_c^2f}{g^2})$. As $A_{\pm}\to0$, we have that $U_2\approx1$ and state of the superradiant phases can be approximated as

$$|\psi\rangle_{\mathrm{sp}}\approx\prod_{n=1}^{3}\tilde{D}_n\prod_{n=1}^{3}\tilde{U}_n|0\rangle_x|0\rangle_p\prod_{n=1}^{3}|-\rangle_n. \tag{C.1}$$

For the '$n=1$' trapped ion, its spin state is changed from $\mathrm{e}^{-i\gamma\sigma_1^{\dagger}\sigma_1^{-}}|-\rangle_1$ to $|g\rangle_1$ by the optical pulse. Thus, we have prepared the system into an initial state

$$|\psi(0)\rangle=\tilde{D}_1\mathrm{e}^{i\gamma a_1^{\dagger}a_1}\prod_{n=2}^{3}\tilde{D}_n\tilde{U}_n|0\rangle_x|0\rangle_p|g\rangle_1\prod_{n=2}^{3}|-\rangle_n. \tag{C.2}$$

Secondly, applying a running wave light field to drive the '$n=1$' trapped ion for various time intervals $\tilde{t}$. Under the resonance condition of first blue sideband [52], its evolution is described by following interaction Hamiltonian

$$H_i=\frac{\hbar\Gamma}{2}\left(a_1^{\dagger}\sigma_1^{\dagger}+a_1\sigma_1^{-}\right) \tag{C.3}$$

with coupling frequency Γ determined by the external light field. At time $\tilde{t}$, wave function of the system evolves into

$$|\psi(\tilde{t})\rangle=\mathrm{e}^{-\frac{i}{\hbar}H_i\tilde{t}}|\psi(0)\rangle=\mathrm{e}^{-\frac{i}{2}\Gamma\tilde{t}\left(a_1^{\dagger}\sigma_1^{\dagger}+a_1\sigma_1^{-}\right)}|\psi(0)\rangle. \tag{C.4}$$

Thirdly, measuring the probability $P_g(\tilde{t})=\langle\psi(\tilde{t})|(|g\rangle_1\langle g|)|\psi(\tilde{t})\rangle$ to find the '$n=1$' trapped ion in its ground state $|g\rangle_1$. We can obtain that

$$\begin{aligned}P_g(\tilde{t})&=\langle\psi(0)|\mathrm{e}^{\frac{i}{\hbar}H_i\tilde{t}}(|g\rangle_1\langle g|)\,\mathrm{e}^{-\frac{i}{\hbar}H_i\tilde{t}}|\psi(0)\rangle\\&={}_p\langle0|_x\langle0|\mathrm{e}^{-i\gamma a_1^{\dagger}a_1}\tilde{D}_1^{\dagger}\,{}_1\langle g|\mathrm{e}^{\frac{i}{\hbar}H_i\tilde{t}}|g\rangle_1\langle g|\mathrm{e}^{-\frac{i}{\hbar}H_i\tilde{t}}|g\rangle_1\tilde{D}_1\mathrm{e}^{i\gamma a_1^{\dagger}a_1}|0\rangle_x|0\rangle_p\\&={}_p\langle0|_x\langle0|\mathrm{e}^{-i\gamma a_1^{\dagger}a_1}\tilde{D}_1^{\dagger}\cos^2\left(\frac{\Gamma\tilde{t}}{2}\sqrt{a_1a_1^{\dagger}}\right)\tilde{D}_1\mathrm{e}^{i\gamma a_1^{\dagger}a_1}|0\rangle_x|0\rangle_p\\&=\frac{1}{2}\left(1+{}_p\langle0|_x\langle0|\mathcal{D}_1^{\dagger}\cos\left(\Gamma\tilde{t}\sqrt{a_1a_1^{\dagger}}\right)\mathcal{D}_1|0\rangle_x|0\rangle_p\right)\\&=\frac{1}{2}\left(1+{}_p\langle0|_x\langle0|\cos\left(\Gamma\tilde{t}\sqrt{a_1a_1^{\dagger}+\alpha\left(a_1^{\dagger}+a_1\right)+\alpha^2}\right)|0\rangle_x|0\rangle_p\right),\end{aligned} \tag{C.5}$$

where we have defined operator $\mathcal{D}_1=\mathrm{e}^{-i\gamma a_1^{\dagger}a_1}\tilde{D}_1\mathrm{e}^{i\gamma a_1^{\dagger}a_1}=\mathrm{e}^{\alpha(a_1^{\dagger}-a_1)}$ and used equations

$$\begin{aligned}{}_1\langle g|\mathrm{e}^{-\frac{i}{\hbar}H_i\tilde{t}}|g\rangle_1&=\sum_m\frac{(-i)^m}{m!}\left(\frac{\Gamma\tilde{t}}{2}\right)^m{}_1\langle g|\left(a_1^{\dagger}\sigma_1^{\dagger}+a_1\sigma_1^{-}\right)^m|g\rangle_1=\sum_m\frac{(-1)^m}{(2m)!}\left(\frac{\Gamma\tilde{t}}{2}\right)^{2m}\left(a_1a_1^{\dagger}\right)^m\\&=\cos\left(\frac{\Gamma\tilde{t}}{2}\sqrt{a_1a_1^{\dagger}}\right),\end{aligned} \tag{C.6}$$

$$\mathcal{D}_1^\dagger \cos\left(\Gamma\tilde{t}\sqrt{a_1 a_1^\dagger}\right)\mathcal{D}_1 = \cos\left(\Gamma\tilde{t}\sqrt{a_1 a_1^\dagger + \alpha\left(a_1^\dagger + a_1\right) + \alpha^2}\right). \tag{C.7}$$

We next express a_1 and $a_1^\dagger$ in momentum space and can acquire that

$$a_1^\dagger + a_1 = \frac{1}{\sqrt{3}}\left[a_0^\dagger + a_0 + (\mu - \nu)\sum_{p\neq 0} \mathrm{e}^{-ip}\left(b_p^\dagger + b_{-p}\right)\right] \tag{C.8}$$

$$\begin{aligned} a_1 a_1^\dagger = &\frac{2}{3}\mu^2 + \frac{1}{3}a_0 a_0^\dagger + \frac{1}{3}\sum_{p\neq 0}([[(\mu^2+\nu^2)b_p^\dagger b_p - \mu\nu(b_p b_{-p} + b_{-p}^\dagger b_p^\dagger)], \\ &+ \mathrm{e}^{-i2p}[(\mu^2+\nu^2)b_{-p}^\dagger b_p - \mu\nu(b_p b_p + b_{-p}^\dagger b_{-p}^\dagger)] \\ &+ a_0^\dagger \mathrm{e}^{-ip}(\mu b_p - \nu b_{-p}^\dagger) + a_0 \mathrm{e}^{ip}(\mu b_p^\dagger - \nu b_{-p})), \end{aligned} \tag{C.9}$$

with which the probability $P_g(\tilde{t})$ can be rewritten as

$$\begin{aligned} P_g(\tilde{t}) = &\frac{1}{2}\Bigg(1 + \sum_m \frac{(-1)^m}{(2m)!}(\Gamma\tilde{t})^{2m}\ {}_p\langle 0|_x\langle 0|\Big[\alpha^2 + \frac{2}{3}\mu^2 \\ &+ \frac{1}{3}a_0 a_0^\dagger + \frac{1}{\sqrt{3}}(a_0^\dagger + a_0) + \cdots\Big]^m |0\rangle_x|0\rangle_p\Bigg) \\ = &\frac{1}{2}\left(1 + \cos(\tilde{\Gamma}\tilde{t}) + \sum_m \frac{(-1)^m}{(2m)!}(\Gamma\tilde{t})^{2m}\ {}_x\langle 0|\left(\frac{1}{3}a_0 a_0^\dagger\right)^m |0\rangle_x + \cdots\right) \\ = &\frac{1}{2}\left(1 + \cos(\tilde{\Gamma}\tilde{t}) + \sum_n \frac{H_n^2(0)}{2^n n!\sqrt{\pi}}\cos(\tilde{\Gamma}_n\tilde{t}) + \cdots\right), \end{aligned} \tag{C.10}$$

where $\tilde{\Gamma} = \sqrt{\alpha^2 + \frac{2}{3}\mu^2}\Gamma$, $\tilde{\Gamma}_n = \sqrt{\frac{n+1}{3}}\Gamma$, $H_n(x)$ is the Hermitian polynomials. In equation (C.10), many cross-terms are hidden in the ellipsis, which can contain plenty of undetermined oscillation frequencies; just as expected, the summation terms are closely related with populations of Fock states $|n\rangle$ in the ground state $|0\rangle_x$ [52], they result in the frequencies $\tilde{\Gamma}_n$ that are decided only by n and Γ; an oscillating term originating from the displacement operator $\tilde{D}_1$ and excitations is also successfully figured out, whose oscillation frequency $\tilde{\Gamma}$ can give us information about α and γ. Thus, in experiments we can verify the three superradiant phases through finding out oscillation frequency $\tilde{\Gamma}$ of the spin evolution probability $P_g(\tilde{t})$.

ORCID iD

Yong-Chang Zhang https://orcid.org/0000-0001-9319-2125

References

[1] Acín A et al 2018 *New J. Phys.* **20** 080201
[2] Giustino F et al 2021 *J. Phys. Mater.* **3** 042006
[3] DiVincenzo D P 2000 *Fortschr. Phys. Prog. Phys.* **48** 771–83
[4] Giovannetti V, Lloyd S and Maccone L 2006 *Phys. Rev. Lett.* **96** 010401
[5] Wang J and Zhang S C 2017 *Nat. Mater.* **16** 1062–7
[6] Rau J G, Lee E K H and Kee H Y 2016 *Annu. Rev. Condens. Matter Phys.* **7** 195–221
[7] Bloch I, Dalibard J and Nascimbene S 2012 *Nat. Phys.* **8** 267–76
[8] Angelakis D G 2017 *Quantum Science and Technology* (Springer) p 134
[9] Paraoanu G S 2014 *J. Low Temp. Phys.* **175** 633–54
[10] Greiner M, Mandel O, Esslinger T, Hänsch T W and Bloch I 2002 *Nature* **415** 39–44
[11] Stöferle T, Moritz H, Schori C, Köhl M and Esslinger T 2004 *Phys. Rev. Lett.* **92** 130403
[12] Hasan M Z and Kane C L 2010 *Rev. Mod. Phys.* **82** 3045
[13] Qi X L and Zhang S C 2011 *Rev. Mod. Phys.* **83** 1057
[14] Sato M and Ando Y 2017 *Rep. Prog. Phys.* **80** 076501
[15] Beenakker C and Kouwenhoven L 2016 *Nat. Phys.* **12** 618–21
[16] Möller G and Cooper N R 2009 *Phys. Rev. Lett.* **103** 105303
[17] Kapit E and Mueller E 2010 *Phys. Rev. Lett.* **105** 215303
[18] Li J, Huang W, Shteynas B, Burchesky S, Top F Ç, Su E, Lee J, Jamison A O and Ketterle W 2016 *Phys. Rev. Lett.* **117** 185301
[19] Hsieh D et al 2009 *Science* **323** 919–22
[20] Cheng J M, Gong M, Guo G C, Zhou Z W and Zhou X F 2019 *New J. Phys.* **21** 123051
[21] Sarma S D, Freedman M and Nayak C 2015 *npj Quantum Inf.* **1** 1–13
[22] Flensberg K, von Oppen F and Stern A 2021 *Nat. Rev. Mater.* **6** 944–58
[23] Flynn V P, Cobanera E and Viola L 2021 *Phys. Rev. Lett.* **127** 245701

[24] Vojta M 2003 *Rep. Prog. Phys.* **66** 2069
[25] Sachdev S 1999 *Phys. World* **12** 33
[26] Bansil A, Lin H and Das T 2016 *Rev. Mod. Phys.* **88** 021004
[27] Zhang D W, Zhu Y Q, Zhao Y, Yan H and Zhu S L 2018 *Adv. Phys.* **67** 253–402
[28] Stoof H T, Gubbels K B and Dickerscheid D B 2009 *Ultracold Quantum Fields* (Springer) pp 193–212
[29] Dimer F, Estienne B, Parkins A and Carmichael H 2007 *Phys. Rev.* A **75** 013804
[30] Viehmann O, von Delft J and Marquardt F 2011 *Phys. Rev. Lett.* **107** 113602
[31] Nataf P and Ciuti C 2010 *Nat. Commun.* **1** 72
[32] Huang J F and Tian L 2022 arXiv:2208.12524
[33] Wu Z, Zhang L, Sun W, Xu X T, Wang B Z, Ji S C, Deng Y, Chen S, Liu X J and Pan J W 2016 *Science* **354** 83–88
[34] Zhang D *et al* 2019 *Phys. Rev. Lett.* **122** 110402
[35] Hwang M J, Puebla R and Plenio M B 2015 *Phys. Rev. Lett.* **115** 180404
[36] Cai M L, Liu Z D, Zhao W D, Wu Y K, Mei Q X, Jiang Y, He L, Zhang X, Zhou Z C and Duan L M 2021 *Nat. Commun.* **12** 1126
[37] Blume D 2012 *Rep. Prog. Phys.* **75** 046401
[38] Ran S J, Piga A, Peng C, Su G and Lewenstein M 2017 *Phys. Rev.* B **96** 155120
[39] Roushan P *et al* 2017 *Nat. Phys.* **13** 146–51
[40] Zhang Y Y, Hu Z-X, Fu L, Luo H-G, Pu H and Zhang X-F 2021 *Phys. Rev. Lett.* **127** 063602
[41] Padilla D F, Pu H, Cheng G J and Zhang Y Y 2022 *Phys. Rev. Lett.* **129** 183602
[42] Solano E, Agarwal G S and Walther H 2003 *Phys. Rev. Lett.* **90** 027903
[43] Rodriguez-Lara B, Moya-Cessa H and Klimov A 2005 *Phys. Rev.* A **71** 023811
[44] Lv D, An S, Liu Z, Zhang J N, Pedernales J S, Lamata L, Solano E and Kim K 2018 *Phys. Rev.* X **8** 021027
[45] Ohira R, Kume S, Takahashi H and Toyoda K 2021 *Quantum Sci. Technol.* **6** 024015
[46] Hayward A L and Martin A M 2016 *Phys. Rev.* A **93** 023828
[47] Koch J, Houck A A, Le Hur K and Girvin S 2010 *Phys. Rev.* A **82** 043811
[48] Burgess C P 2000 *Phys. Rep.* **330** 193–261
[49] Hwang M J and Plenio M B 2016 *Phys. Rev. Lett.* **117** 123602
[50] Colpa J 1978 *Physica* A **93** 327–53
[51] Moya-Cessa H M and Eguibar F S 2013 arXiv:1309.0140
[52] Leibfried D, Blatt R, Monroe C and Wineland D 2003 *Rev. Mod. Phys.* **75** 281
[53] Colpa J 1986 *Physica* A **134** 417–42